communications biology

A Nature Portfolio journal

Article

https://doi.org/10.1038/s42003-025-07671-2

GINNA, a 33 resting-state networks atlas with meta-analytic decoding-based cognitive characterization

Achille Gillig, Sandrine Cremona, Laure Zago, Emmanuel Mellet, Michel Thiebaut de Schotten, Marc Joliot ✉ & Gael Jobard

Since resting-state networks were first observed using magnetic resonance imaging (MRI), their cognitive relevance has been widely suggested. However, to date, the empirical cognitive characterization of these networks has been limited. The present study introduces the Groupe d'Imagerie Neurofonctionnelle Network Atlas, a comprehensive brain atlas featuring 33 resting-state networks. Based on the resting-state data of 1812 participants, the atlas was developed by classifying independent components extracted individually, ensuring consistent between-subject detection. We further explored the cognitive relevance of each GINNA network using Neurosynth-based meta-analytic decoding and generative null hypothesis testing. Significant cognitive terms for each network were then synthesized into appropriate cognitive processes through the consensus of six authors. The GINNA atlas showcases a diverse range of topological profiles, reflecting a broad spectrum of the known human cognitive repertoire. The processes associated with each network are named according to the standard Cognitive Atlas ontology, thus providing opportunities for empirical validation.

The brain is intrinsically organized into sets of tightly coupled brain regions or networks. Using resting-state functional magnetic resonance imaging (rs-fMRI), it has been observed that distant brain regions display synchrony in their low-frequency spontaneous fluctuations of the blood oxygen level-dependent (BOLD) signal[1]. Understanding the functional role of these so-called resting-state networks (RSNs) remains a central goal of cognitive neuroscience. It has long been posited that the coordinated activity of distributed brain regions supports cognition[2–4]. Since their first observations, it has been noted that RSNs follow an organization reflecting the boundaries of the main cognitive systems observed during tasks—e.g., somatomotor[1], vision[5], episodic memory[6], language[7] - suggesting that RSNs may represent functionally relevant systems[8–10]. However, while it has been suggested that networks should be named according to an anatomically grounded taxonomy[11], researchers tend to name networks according to their putative cognitive functions[12].

Initially, the brain at rest has been proposed to be intrinsically segregated into two anticorrelated extrinsic, "task-positive", and intrinsic, "task-negative" systems[13]. Later, it was shown that these two systems could be hierarchically decomposed into five modules, thought to subserve distinct functions: switching/control, sensory/motor/attentional, visual, manipulation/maintenance of information, and the emergence of spontaneous thoughts[14]. Finally, the currently most widely used atlas proposes segregation into seven functional networks: visual, somatomotor, dorsal attention, ventral attention (salience), limbic, frontoparietal (control), and default network[15]. Yet, the functional relevance of RSNs remains indirectly established: such cognitive functions of networks have been inferred because of a visual similarity with task-based networks. This method of deducing a functional role for a given network based on visual similarity alone has been shown to be poorly reliable, even when performed by neuroimaging specialists[12]. This can be particularly problematic given that these inferred cognitive functions are frequently used to interpret results. Further complicating the association of cognitive functions to resting-state networks, it has been suggested that there may not be a clear one-to-one mapping between large-scale networks and cognitive processes with the low granularity (i.e., seven networks) typically observed in RSN atlases[16].

Nonetheless, several lines of empirical evidence have supported the cognitive relevance of RSNs. The first direct link between the organization of the resting brain and the brain undergoing tasks was made by Smith et al. (2009)[17] showing that networks extracted using independent component analysis (ICA) at rest closely matched spatially networks extracted using the same methodology from the BrainMap activation maps database[18]. Since this seminal observation, numerous studies have reinforced the link between resting-state and task-based network architectures, providing evidence that the network architecture observed during tasks is shaped by resting-state networks' architecture[19,20], or that resting-state networks implement cognition modularly[21,22]. All in all, this supports the claim that resting-state networks may reflect critical cognitive units.

GIN, IMN-UMR5293, Université de Bordeaux, CEA, CNRS, Bordeaux, France. ✉e-mail: marc.joliot@u-bordeaux.fr

Laird et al. (2011)[23] were the first to deliver an extensive description of the cognitive interpretation of intrinsic connectivity networks. Using the same methodology as in Smith et al. (2009)[17] (i.e., ICA) to derive intrinsic connectivity networks from the BrainMap database[18], these interpretations were made possible thanks to the richness of the manual annotations provided in the database relative to cognitive processes. In a similar attempt, another study used the BrainMap taxonomy[18] to extract the "functional fingerprint" of networks across 20 cognitive domains (e.g., "Audition-Perception", "Memory-Cognition"), allowing to reveal each network's unique cognitive profile[24]. However, despite the highly valuable insights provided by these studies, some limitations appear. For instance, while links to cognitive-behavioral terminology were made possible by analyzing network maps derived from task studies[17,23], the interpretation of RSN was still inferred from their apparent resemblance to the BrainMap-derived (i.e., task-based) networks. This approach carries the risk that minor differences in topology or regional activation levels could lead to significant differences in their respective cognitive profile. Alternatively, other studies defined each network's cognitive profile according to 20 broad behavioral domains[24], therefore dampening the fine description of the involved cognitive processes. Finally, despite the high metadata quality of the activation maps found in the BrainMap database, these metadata come from manual annotations of a subset of the available studies, therefore preventing it from incorporating a large part of the fMRI literature. By contrast, relying on natural language processing, Neurosynth[25] is a database that relies on the automatic generation of term-related meta-analytic maps from thousands of fMRI activation studies. Therefore, compared to BrainMap, it scales much more extensively and encompasses more specific terms than BrainMap's broad behavioral domains.

More recently, building on the development of Neurosynth[25], a new class of decoding methods has emerged to probe the potential involvement of cognitive functions given some brain activity[26–28]. Such decoding methods can be used to infer the presence of putative cognitive processes by spatial comparison to meta-analytic maps. For instance, meta-analytic decoding has been successfully used to infer the cognitive content of short task-fMRI blocks[29], or to reveal the cognitive profiles of the human intraparietal sulcus[30] or the cognitive states of participants watching a video[31]. These methods can potentially assess the cognitive relevance of RSNs by allowing the statistical comparison of their topology to meta-analytic maps. However, to the best of our knowledge, meta-analytic decoding has never been applied for the characterization of the potential cognitive relevance of RSNs.

The present study introduces the Groupe d'Imagerie Neurofonctionnelle Network Atlas (GINNA), a new fine-grained 33 networks atlas with an empirical characterization of each network's cognitive relevance. Contrasting with existing atlases, GINNA creation relied on the classification of independent components obtained at the individual level, providing finer granularity and ensuring that components are reliably present across individuals. We developed a strategy for attributing cognitive labels to networks relying on decoding cognitive terms from a manually curated subset of the Neurosynth database, therefore providing an exhaustive characterization of their putative cognitive functions in light of the current neuroimaging literature. Such an atlas grounded in a careful characterization of its putative cognitive functions could be a useful guide when combined with newly emerging methods, allowing the reveal of mechanistic accounts in future direct/causal assessments of large-scale networks' functions.

Results

GINNA resting-state networks

The GINNA atlas is presented in Fig. 1 and Fig. 2, and is made publicly available at https://github.com/Achillegillig/ginna[32]. The procedure of resting-state network (RSN) decomposition resulted in 41 networks. Out of the 41 RSNs identified by the procedure, 7 that did not overlap the brain (mainly venous artifacts), as well as one limited to the brainstem, were excluded from further analyses, resulting in a total of 33 RSNs further analyzed. The RSNs numbering (RSN01 to RSN33) reflects the reliability of their identification: RSNs with the lowest numbering are detected in most subjects (highest between-subject reliability), with RSN01 being detected in 99.94% and RSN33 in 49.59% of participants. The GINNA atlas covers an estimated 90% of the cortex as defined by the SPM gray matter template (Supplementary Fig. 1). Voxels that are not covered are within areas sensitive to susceptibility artifacts[33] and distortions. The former are in the orbito-frontal cortex (directly above the frontal sinus), and inferior temporal region above the ear canals. The latter occurs in the frontal part of the brain due to signal loss linked to the phase encoding that was set in the anterior-posterior axis[34]. Note that the applied distortion correction did, in fact, recover some signal but not all[35], since it falls outside the acquired k-space. From the 6 networks not included in the analysis, one was comprised of the major part of the not-covered orbito-frontal areas, its annular geometry was compatible with the susceptibility artifacts and furthermore included regions out of the brain in the CSF crown. We thus considered that it didn't qualify as a network and was not included in the analysis. Notably, the least detected RSN33 encompasses a substantial portion of the anterior and inferior temporal lobe regions. Thus, susceptibility likely contributes to the lower individual subject detectability of RSN33 in our atlas.

The replication of the group-average RSN creation using a gender-balanced subsample of 1016 subjects ($n = 508$ female) indicated a near-perfect correspondence with the original GINNA Atlas, as assessed using the Dice coefficient (mean ± s.d.: 0.96 ± 0.01; range: [0.92–0.98]) (Supplementary Figs. 2 and 3). Females and males in the gender-balanced subsample did not significantly differ in age (two-tailed t-test; $t(1013.48) = 0.305$, $p = 0.76$). In addition, a replication of the RSNs creation procedure on a subset of 150 subjects from the HCP dataset[36] balanced for gender demonstrated that 28 of the 32 cortical RSNs were reproducibly identified in both datasets (Supplementary Figs. 4 and 5) Notably, the four networks not observed in the HCP-based analysis (RSN18, RSN27, RSN31, RSN33) were among those least frequently detected in the larger dataset, likely reflecting the smaller sample size selected from the HCP cohort.

Meta-analytic cognitive terms decoding

Out of the 506 meta-analytic maps, 241 (47.6%) were not decoded for any RSN (Supplementary Fig. 6A). Terms that were not significant across all RSNs were characterized by maps with a greater number of null values than maps decoded at least for one RSN (Supplementary Fig. 6B). The least associated terms (i.e., non-significant terms with the lowest Pearson r with any RSN) were distributed in the emotional domain (Supplementary Fig. 6C). Our procedure allowed to identify an average of 12 terms per network, with associations ranging from 38 ($n = 1$; RSN32) to 0 terms ($n = 3$; RSNs 01, 02, 26) (Fig. 3, Table 1). The MAMs correlating significantly with their respective RSNs resulted in an average correlation of $r = 0.61$, with a maximum of $r = 0.91$ (RSN14) and a minimum of $r = 0.32$ (RSN31) (Fig. 3). Detailed results for each network are available in the supplementary materials (Supplementary Figs. 7–39).

Resting-state network's cognitive labeling

Consensus cognitive labeling. The cognitive processes that emerged from the expert's consensus for each network, corresponding to Cognitive Atlas concepts[37], are presented in Table 2, Fig. 1 and Fig. 2. The attributed processes covered a large span of cognitive functions. This included sensory and motor functions, with auditory ($n = 1$; TN-01 (RSN14)—auditory perception), somatomotor ($n = 5$; PcN-01 (RSN06)—movement (limb); PcN-02 (RSN04)—articulation; PcN-03 (RSN11)—somatosensation; R-PcN (RSN25)—movement (left hand); L-PcN (RSN21)—movement (right hand)), and visual processes ($n = 4$; ON-01 (RSN09)—visual perception; ON-02 (RSN29)—visual form discrimination ON-04 (RSN03)—motion detection, visual object recognition; OTN (RSN32)—object perception). We also uncovered several resting-state networks related to more integrated visuomotor and visuospatial processes ($n = 3$; D-FPN-01 (RSN10)—motor planning; D-FPN-02 (RSN30)—motor imagery; D-FPN-03 (RSN08)—spatial selective attention).

We also evidenced RSNs related to other high-level cognitive processes ($n = 5$; R-FTPN-02 (RSN20)—mental arithmetic; L-InsFPN (RSN23)—phonological working memory; L-FTPN-02 (RSN12)—reasoning; mCingFPN

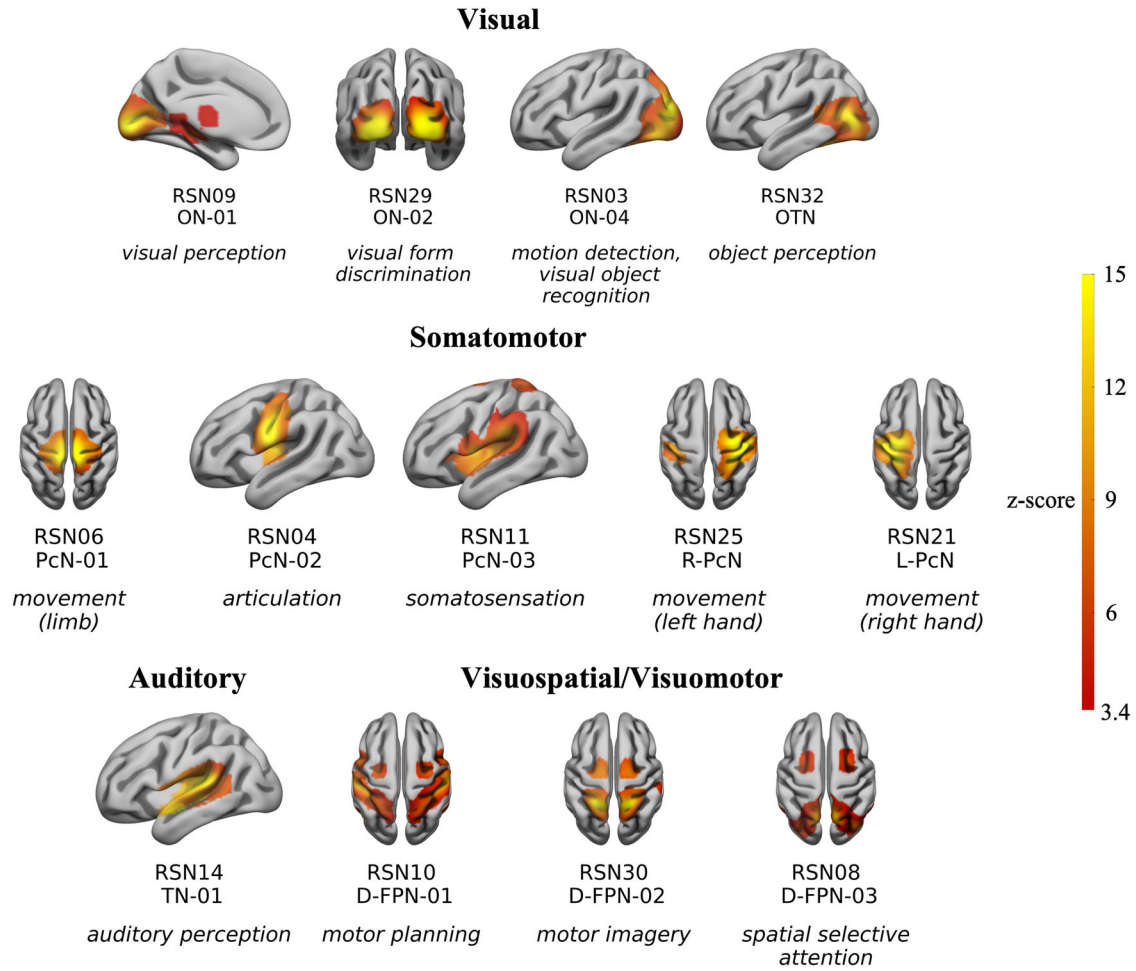

Fig. 1 | GINNA resting-state networks associated with sensory and motor-related processes. Each resting-state network is presented as a projection on a 3D view of the brain accompanied by its numbering (top), anatomical nomenclature (middle), and suggested cognitive process(es) (bottom). RSNs without significantly decoded terms (n.s.) were positioned in a "non-significant" category (see Fig. 3). The Color scale is mapped to the *z*-scores of each RSN ICA component. Abbreviations: D dorsal, F frontal, L left, N network, n.s. non-significant, O occipital, P parietal, Pc pericentral, R right, T temporal. For illustration purposes, only the most representative view of each RSN is shown, refer to the Supplementary Figs. for a more complete depiction.

(RSN16)—working memory; FTPN-02 (RSN27)—reading, mental arithmetic). Other high-level processes included cognitive control ($n = 3$; R-FInsN (RSN31)—cognitive control; mCingInsN (RSN22)—performance monitoring; FTPN-01 (RSN18)— expectancy), decision-making ($n = 2$; BGN (RSN24)—reward anticipation; aCingN (RSN13)— decision making).

Three networks were associated with language-related terms, two of which were strongly left-lateralized (L-FTN (RSN15)—syntactic processing; L-FTPN-01 (RSN19)—sentence comprehension), and another encompassing the bilateral temporal gyrus (TN-02 (RSN33)—speech perception). In addition, two networks were associated with social cognition ($n = 2$: med-FN (RSN28)—theory of mind; R-FTPN-01 (RSN17)—self-monitoring, theory of mind).

Two networks were related to the default mode, as evidenced by a significant decoding of the terms "default mode" and "default network", and were associated with memory ($n = 1$; med-TN (RSN05)—memory retrieval); and thoughts about the self ($n = 1$; med-FPN (RSN07)—self-referential processing).

RSNs for which the meta-analytic decoding procedure did not result in any significant association with meta-analytic maps ($n = 3$; pCing-medPN (RSN01), R-FTPN-03 (RSN02), ON-03 (RSN26)), were labeled as non-significant (*n*.s.).

Latent semantic cognitive labeling. Cognitive labels obtained from the fully data-driven latent semantic analysis-based procedure (LSA) are presented in Table 2. As compared with the cognitive labels manually derived by the experts, the data-driven labels generally refer to similar cognitive domains. The most notable exceptions are RSN07, associated with self-referential processing (experts-driven label) vs divergent thinking (LSA label), and RSN29 (visual form discrimination vs. task difficulty). While the cognitive domains generally agree, the level of specification varies with subprocesses being sometimes put forward by the LSA labeling compared to the consensus labeling: RSN20, labeled as spatial working memory vs. mental arithmetic, RSN21 motor planning vs. movement; RSN28 inference vs. theory of mind; RSN33 auditory sentence comprehension vs. speech perception.

Detailed results for default mode and language networks. In this section, we focus on a few networks that illustrate well how our results relate to the state of the art and how the results from the principal component analyses were used as a basis for the consensus among authors to choose the cognitive labels. Exhaustive results for each RSN are available in the supplementary materials.

Default mode networks: RSN05, 07—med-TN, med-FPN. Two networks were associated with terms related to the default mode ("default network", "default mode"): RSN05 (med-TN) and RSN07 (med-FPN) (Fig. 4).

RSN05 (med-TN) encompassed the hippocampal gyri, posterior cingulum, precuneus, and bilateral angular gyri. In addition to terms related to

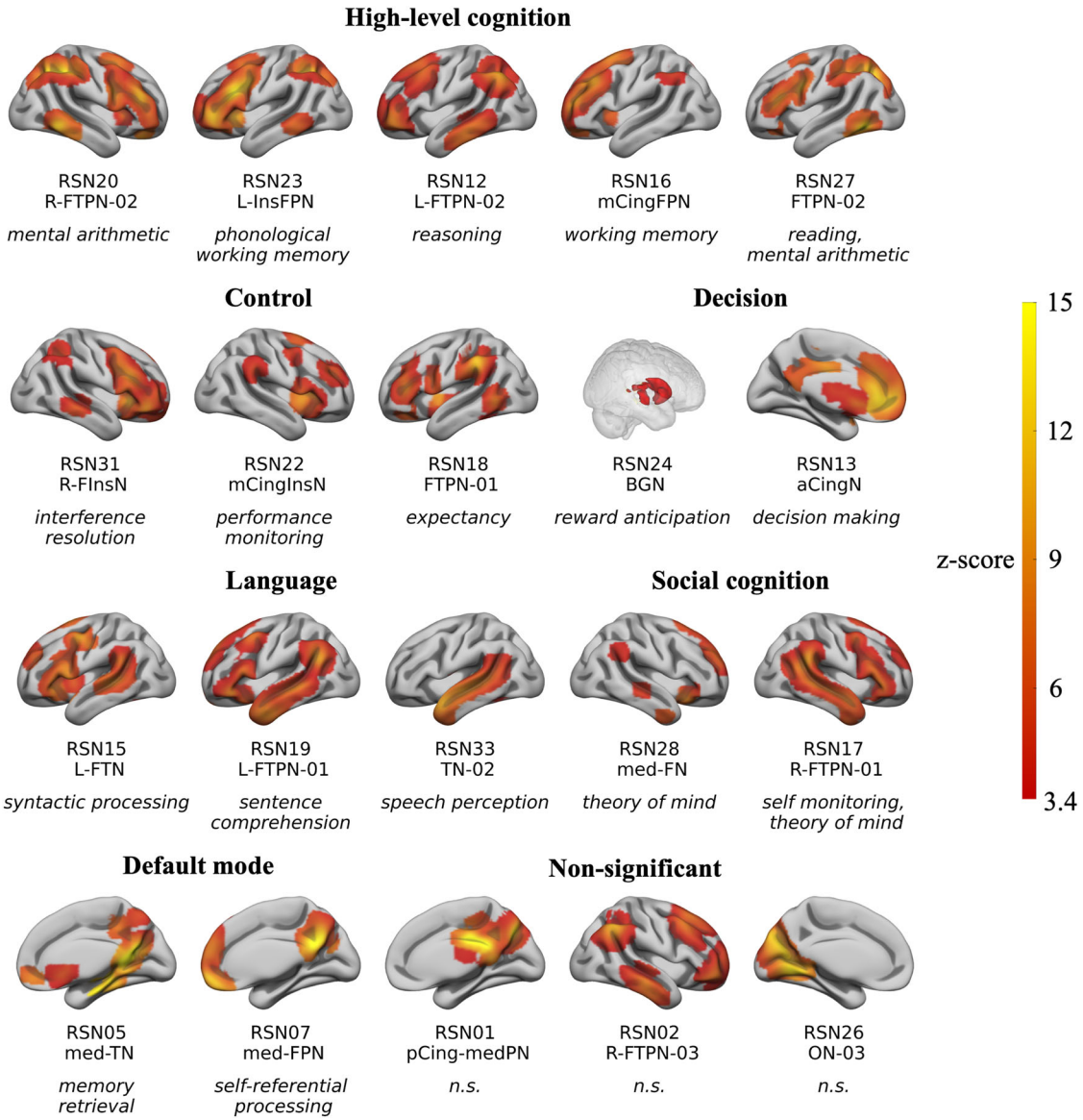

Fig. 2 | GINNA networks associated with higher-level processes and non-significant networks. Each resting-state network is presented as a projection on a 3D view of the brain accompanied by its numbering (top), anatomical nomenclature (middle), and suggested cognitive process(es) (bottom). RSNs without significantly decoded terms (n.s.) were positioned in a "non-significant" category. The color scale is mapped to the z-scores of each RSN ICA component. Abbreviations: BG basal ganglia, a/m/pCing anterior/middle/posterior cingulate, D dorsal, F frontal, Ins insular, L left, med median, N network, n.s. non-significant, O occipital, P parietal, R right, T temporal. For illustration purposes, only the most representative view of each RSN is shown, refer to the Supplementary Figs. for a more complete depiction.

the default mode, RSN05 was associated with terms related to memory, with the three most correlated terms referring to autobiographical aspects of declarative memory (autobiographical memory: $r = 0.71$, $p < 0.001$; episodic: $r = 0.66$, $p < 0.001$; autobiographical: $r = 0.64$, $p < 0.001$; Table 1, Fig. 4). The cognitive label resulting from the consensus for this RSN was "memory retrieval" (Table 2).

RSN07 (med-FPN) comprised the medial prefrontal cortex (mPFC), posterior cingulate cortex (PCC), precuneus, and the bilateral angular gyri, therefore corresponding to the canonical anatomical definition of the default mode network (DMN). Seventeen terms were decoded for this network. Unsurprisingly, the two most correlated terms referred to the default mode (default mode: $r = 0.84$, $p < 0.001$; default network: $r = 0.72$, $p < 0.001$) (Table 1, Fig. 4). The principal component analysis computed on the network regions' meta-analytic activations indicated that the terms significantly associated with the network could be summarized in two principal components (PCs) that explained 41.6% and 20.7% of the variance, respectively (Supplementary Fig. 13). PC1 loaded positively on all terms that generally referred to internal thoughts (with theory of mind and mentalizing at the top of the loadings), while PC2 represented an opposition between thoughts oriented to one owns' experience (autobiographical memory, self-referential, personal) and thoughts associated to a more social context (beliefs, moral, social). The consensus cognitive process that emerged for this network was "self-referential processing".

Language networks: RSN15, 19, 33—L-FTN, L-FTPN-01, TN-02. The three networks associated with language processes were L-FTN (RSN15) and L-FTPN-01 (RSN19), lateralized to the left hemisphere, and TN-02 (RSN33), encompassing the superior temporal gyri and extending ventrally in the middle temporal gyri of both hemispheres (Fig. 5). Anatomically, all three networks overlapped in a region centered on the posterior part of the left superior temporal sulcus (STS), extending in the superior and middle temporal gyri. In addition, L-FTN and L-FTPN-01 displayed a partial overlap in the inferior frontal gyrus, the precentral sulcus, and the superior frontal gyrus, with L-FTPN-01 always more

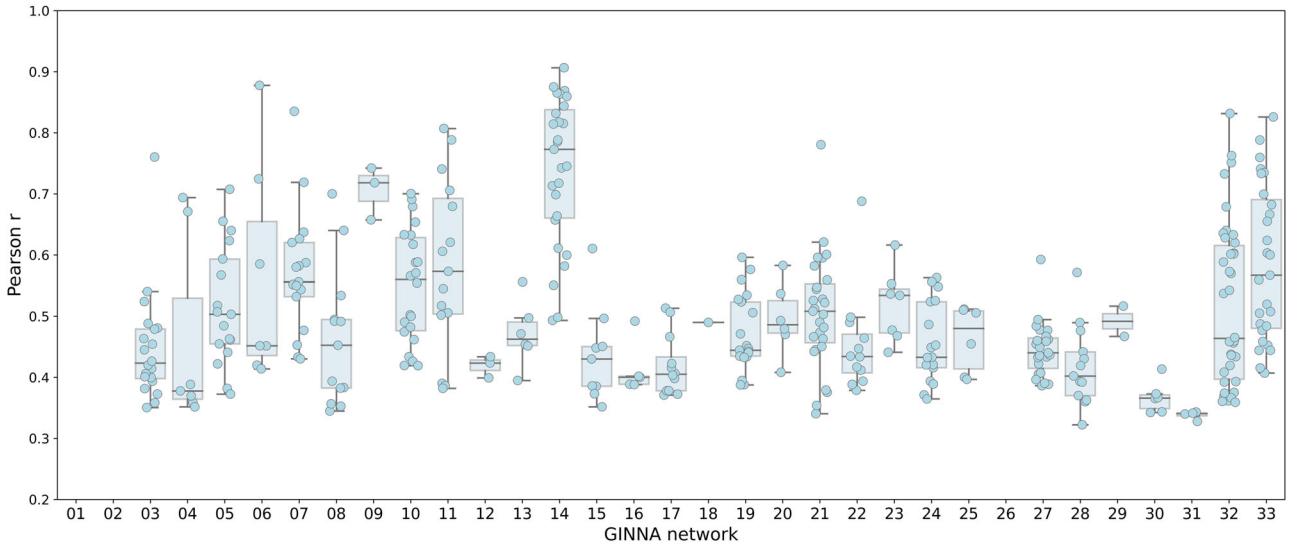

Fig. 3 | Meta-analytic decoding. Distribution of significant Pearson correlations between each GINNA network and Neurosynth meta-analytic maps. The middle line indicates the median. Boxes indicate the 1st and 3rd quartiles. Whiskers indicate the min-max range of r values, excluding outliers.

anterior than L-FTN. L-FTPN-01 extended also more posteriorly in the left angular gyrus, while the L-FTN stopped in the supramarginal gyrus. The cognitive terms significantly associated with TN-02 grouped into two cognitive principal components (Supplementary Fig. 39), with a first component (56.5% explained variance) regrouping terms related to the auditory modality (spoken, listening, speech, auditory, acoustic). The second component (24.3% explained variance) opposed the comprehension of language (sentence comprehension, language network) to its less linguistic dimension (communication, sounds, acoustic). High positive loadings were most present in the left hemisphere STS and middle temporal regions and strong negative loadings were observed in the bilateral superior temporal gyri and the right STS and right middle temporal gyrus (Supplementary Fig. 39). TN-02 was labeled as "speech perception" with respect to the cognitive atlas terminology.

Though L-FTN and L-FTPN-01 at least partially overlapped, their respective set of associated terms differed. L-FTN, attributed to "syntactic processing", was explained by a single unitary component (90.7% explained variance) most represented by the term's verbs, syntactic, and sentence comprehension (Supplementary Fig. 21). L-FTPN-01, for which was attributed "sentence comprehension", comprised a main component (56.4% explained variance) related to linguistic aspects of language comprehension (language comprehension, sentence comprehension, syntactic, semantic), and a minor one (12.3% explained variance) related to the representation of meaning (mentalizing, theory of mind, inference). The first component was best represented in the left STS and anterior part of the inferior frontal gyrus, while the second was best represented in the left angular gyrus, temporal pole, and anterior part of the medial frontal gyrus (Supplementary Fig. 25).

Discussion

The cognitive relevance of resting-state networks (RSNs) is poorly understood. To help resolve this issue, we propose the Groupe d'Imagerie Neurofonctionnelle Network Atlas (GINNA), a comprehensive RSN atlas derived from the resting-state data of 1812 participants, providing an exhaustive cognitive characterization of the human brain into 33 distinct networks reliably detected at the individual level.

We systematically analyzed the topographical similarities between GINNA networks and meta-analytic maps extracted from the Neurosynth database[25]. Although the method we propose relies on a simple measure of spatial similarity using Pearson correlation, here, we demonstrate its usefulness for investigating the cognitive processes potentially linked to RSNs. By relying on an approach of quantitative meta-analytic decoding of cognitive terms related to GINNA RSNs, we provide an empirically informed cognitive characterization of RSNs. Comparing task-derived meta-analytic maps from the literature and RSNs is particularly relevant if we consider that RSNs represent the prospective exploration of an available repertoire of cognitive functions[38]. In addition, in the context of multivariate pattern analysis, decoding from Neurosynth-derived maps has been shown to perform similarly to more complex, multivariate decoders[39], and to allow to decode from short blocks of task fMRI the cognitive domains that a single participant was engaged in[29]. This suggests that despite its simplicity and low computational cost, decoding based on topographical similarity with activation maps is theoretically justified.

To date, existing brain network parcellations that provide cognitive labeling (e.g., Yeo et al.[15]) have performed an association of function from visual similarity with networks obtained using task paradigms, a method that has proven to result in poor identifiability of RSNs[12]. Alternatively, it has been suggested that networks should be labeled according to their anatomical profile[11]. GINNA RSNs are provided with an anatomically grounded taxonomy accompanied by suggested cognitive process(es) to reconcile both views. Previous attempts of empirical cognitive characterization of RSNs have relied on the analysis of topographically similar task-based networks as a proxy[23], or have done so with respect to broad cognitive domains extracted from BrainMap[24]. By contrast, our assessment of networks obtained at rest benefits from the single cognitive term precision enabled by Neurosynth.

Positioning RSNs cognitive characterization with respect to specific cognitive processes is a much-needed endeavor for the field of cognitive neuroscience. For one, this reference to well-defined psychological constructs allows us to empirically test the predictions we make for each RSN, contrasting with broad cognitive domains ("visual", "control") that are not always informative. Second, as the rationale behind the inference of functions rests upon comparison with the neuroimaging literature, the present cognitive characterization attempts to summarize the current knowledge in both the conceptualization of cognitive concepts (as reflected by the terms present in studies and extracted by Neurosynth), as well as their brain underpinnings (as reflected by the topology of the meta-analytic maps). As such, if the goal is to understand the brain organization of cognition, it may prove more useful to describe RSNs' putative processes in terms related to those used in cognitive theories (e.g., theory of mind, visual perception) rather than using broad terms that do not necessarily relate to any psychological reality (e.g., limbic, visual). Moreover, because almost all attributed processes are referenced in the Cognitive Atlas Ontology (with the exception of "self-referential processing", for which we found no equivalent), users can refer to the definitions provided in order to disambiguate the

Table 1 | Resting-state network reliability and meta-analytic decoding

RSN	Detection (% sub.)	Sig. terms (*n*)	Three closest terms (Pearson *r*, *p*)
01	99.94	0	mnemonic ($r = 0.40$, $p = 0.07$); retrieval ($r = 0.38$, $p = 0.1$); recollection ($r = 0.37$, $p = 0.1$)
02	97.85	0	monitoring ($r = 0.32$, $p = 0.1$); signal_task ($r = 0.29$, $p = 0.2$); cognitive_control ($r = 0.28$, $p = 0.4$)
03	97.46	20	**visual** ($r = 0.76$, $p < 0.001$); **visual_field** ($r = 0.54$, $p < 0.001$); **attended** ($r = 0.52$, $p < 0.001$)
04	96.75	7	**speech_production** ($r = 0.69$, $p < 0.001$); **oral** ($r = 0.67$, $p < 0.001$); **naming** ($r = 0.39$, $p = 0.01$)
05	96.30	17	**autobiographical_memory** ($r = 0.71$, $p < 0.001$); **episodic** ($r = 0.66$, $p < 0.001$); **autobiographical** ($r = 0.64$, $p < 0.001$)
06	96.30	7	**foot** ($r = 0.88$, $p < 0.001$); **limb** ($r = 0.72$, $p < 0.001$); **arm** ($r = 0.59$, $p < 0.001$)
07	94.93	17	**default_mode** ($r = 0.84$, $p < 0.001$); **default_network** ($r = 0.72$, $p < 0.001$); **self_referential** ($r = 0.64$, $p < 0.001$)
08	93.82	13	**spatial** ($r = 0.70$, $p < 0.001$); **orienting** ($r = 0.64$, $p < 0.001$); **visuospatial** ($r = 0.53$, $p < 0.001$)
09	91.56	3	**early_visual** ($r = 0.74$, $p < 0.001$); **primary_visual** ($r = 0.72$, $p < 0.001$); **visual_stimulus** ($r = 0.66$, $p < 0.001$)
10	90.24	22	**hands** ($r = 0.70$, $p < 0.001$); **action_observation** ($r = 0.69$, $p < 0.001$); **action** ($r = 0.68$, $p < 0.001$)
11	89.08	15	**secondary_somatosensory** ($r = 0.81$, $p < 0.001$); **painful** ($r = 0.79$, $p < 0.001$); **noxious** ($r = 0.74$, $p < 0.001$)
12	87.92	3	**reasoning** ($r = 0.43$, $p = 0.02$); **judgments** ($r = 0.42$, $p = 0.03$); **solving** ($r = 0.40$, $p = 0.05$)
13	87.42	6	**money** ($r = 0.56$, $p < 0.001$); **preferences** ($r = 0.50$, $p = 0.001$); **decision_making** ($r = 0.47$, $p = 0.004$)
14	86.93	27	**pitch** ($r = 0.91$, $p < 0.001$); **musical** ($r = 0.88$, $p < 0.001$); **auditory** ($r = 0.87$, $p < 0.001$)
15	86.43	9	**verb** ($r = 0.61$, $p < 0.001$); **verbs** ($r = 0.50$, $p < 0.001$); **syntactic** ($r = 0.45$, $p = 0.002$)
16	85.49	5	**memory_load** ($r = 0.49$, $p = 0.002$); **wm** ($r = 0.40$, $p = 0.03$); **memory_wm** ($r = 0.40$, $p = 0.03$)
17	84.56	12	**nogo** ($r = 0.51$, $p < 0.001$); **response_inhibition** ($r = 0.51$, $p < 0.001$); **intentions** ($r = 0.47$, $p = 0.002$)
18	83.73	1	**expectancy** ($r = 0.49$, $p = 0.002$); response_inhibition ($r = 0.28$, $p = 0.4$); tools ($r = 0.26$, $p = 0.5$)
19	82.46	21	**read** ($r = 0.60$, $p < 0.001$); **sentence** ($r = 0.58$, $p < 0.001$); **comprehension** ($r = 0.56$, $p < 0.001$)
20	82.29	6	**calculation** ($r = 0.58$, $p < 0.001$); **subtraction** ($r = 0.54$, $p < 0.001$); **arithmetic** ($r = 0.49$, $p = 0.003$)
21	75.73	27	**index_finger** ($r = 0.78$, $p < 0.001$); **hand_movements** ($r = 0.62$, $p < 0.001$); **hand** ($r = 0.60$, $p < 0.001$)
22	75.01	12	**conflict** ($r = 0.69$, $p < 0.001$); **stop_signal** ($r = 0.50$, $p < 0.001$); **error** ($r = 0.49$, $p < 0.001$)
23	74.63	7	**demands** ($r = 0.62$, $p < 0.001$); **verbal** ($r = 0.55$, $p = 0.005$); **judgment** ($r = 0.54$, $p = 0.007$)
24	74.30	17	**gain** ($r = 0.56$, $p < 0.001$); **monetary** ($r = 0.56$, $p < 0.001$); **anticipation** ($r = 0.55$, $p < 0.001$)
25	73.52	6	**hand** ($r = 0.51$, $p = 0.003$); **hands** ($r = 0.51$, $p = 0.004$); **motor_task** ($r = 0.51$, $p = 0.004$)
26	72.86	0	integrate ($r = 0.35$, $p = 0.2$); early_visual ($r = 0.29$, $p = 0.5$); visual_stimulus ($r = 0.27$, $p = 0.6$)
27	67.24	23	**arithmetic** ($r = 0.59$, $p < 0.001$); **orthographic** ($r = 0.49$, $p = 0.002$); **judgment** ($r = 0.48$, $p = 0.003$)
28	65.20	13	**inferences** ($r = 0.57$, $p < 0.001$); **judgments** ($r = 0.49$, $p < 0.001$); **mentalizing** ($r = 0.48$, $p < 0.001$)
29	62.11	2	**matching** ($r = 0.52$, $p < 0.001$); **matching_task** ($r = 0.47$, $p = 0.004$); face ($r = 0.33$, $p = 0.1$)
30	61.11	6	**pointing** ($r = 0.41$, $p = 0.003$); **movements** ($r = 0.37$, $p = 0.01$); **imitation** ($r = 0.37$, $p = 0.01$)
31	60.56	4	**cognitive_control** ($r = 0.34$, $p = 0.02$); **interference** ($r = 0.34$, $p = 0.02$); **conflicting** ($r = 0.34$, $p = 0.02$)
32	54.38	38	**motion** ($r = 0.83$, $p < 0.001$); **visual_motion** ($r = 0.76$, $p < 0.001$); **viewing** ($r = 0.75$, $p < 0.001$)
33	49.59	27	**comprehension** ($r = 0.83$, $p < 0.001$); **sentences** ($r = 0.79$, $p < 0.001$); **language_comprehension** ($r = 0.76$, $p < 0.001$)

For each GINNA resting-state network, the Proportion of participants for which the Independent Component was detected at the individual level by the classification procedure, the number of significantly decoded terms, and the three most correlated terms. Bold typeface indicates significance after correction for multiple comparisons ($p_{fwer} < 0.05$). RSNs are ordered by their decreasing order of detection.

meaning of the concept and provide a common ground to all researchers[37]. Cognitive atlas definitions are available in the supplementary materials, as well as at https://www.cognitiveatlas.org/concepts/categories/all.

The proposed atlas contrasts with existing atlases in their granularity; though rarely considered, this finer granularity might prove beneficial. This is supported by evidence showing that when grouping together a large span of networks constructs taken from psychology (e.g., "fear network", "working memory network") into higher-order, large-scale networks, markedly dissimilar cognitive processes become regrouped together[16]. Additionally, while functional lateralization of brain circuits is a crucial organizational principle of the human brain, most existing atlases propose networks that are organized bilaterally. Here, bilateral RSNs are still observed, but the finer granularity in GINNA also resulted in the fragmentation of some bilateral networks into homotopical counterparts. For instance, the hand somatomotor system is fragmented into two homotopical systems that correspond to the somatomotor homunculus of left-hand and right-hand motricity. The same can be observed for other networks, such as the fronto-temporo-parietal networks, that fragment into left and right counterparts, associated with distinct processes (e.g., L-FTPN01: sentence comprehension and R-FTPN01: self-monitoring-theory of mind). The identification of lateralized RSNs in GINNA supports the idea that they represent relevant functional units.

The cognitive processes attributed to GINNA RSNs range from low-order sensorimotor (visual, auditory, sensorimotor), up to more integrated, higher-order domains (decision-making, control, memory, social cognition, language, executive). This high diversity suggests that the GINNA atlas covers an extensive share of the known human cognitive repertoire. Of note, only 3 RSNs could not be significantly associated with any Neurosynth term. More importantly, though different in many aspects from existing atlases, some RSNs of the presently proposed atlas align with some of the main large-scale networks described in the literature[11]. The closest resemblance is observed for RSNs related to the visual (ON-01 to ON-04, OTN), somatomotor (PcN-01 to PcN-03, L-PcN, R-PcN), and default mode systems (med-TN, med-FPN, pCing-medPN). D-FPN-03—RSN08 associated with

Table 2 | Anatomical and cognitive labels of GINNA networks

RSN	Anatomical label	Cognitive Atlas Label	
		Experts	Latent semantic analysis
01	pCing-medPN	n.s.	–
02	R-FTPN-03	n.s.	–
03	ON-04	motion detection, visual object recognition	visual form discrimination
04	PcN-02	articulation	speech production
05	med-TN	memory retrieval	memory retrieval
06	PcN-01	movement (limb)	motor program
07	med-FPN	self-referential processing	divergent thinking
08	D-FPN-03	spatial selective attention	spatial selective attention
09	ON-01	visual perception	visual masking
10	D-FPN-01	motor planning	motor planning
11	PcN-03	somatosensation	nociception
12	L-FTPN-02	reasoning	analogical reasoning
13	aCingN	decision making	decision making
14	TN-01	auditory perception	auditory tone perception
15	L-FTN	syntactic processing	language comprehension
16	mCingFPN	working memory	working memory maintenance
17	R-FTPN-01	self monitoring, theory of mind	response inhibition
18	FTPN-01	expectancy	expectancy
19	L-FTPN-01	sentence comprehension	text comprehension
20	R-FTPN-02	mental arithmetic	spatial working memory
21	L-PcN	movement (right hand)	motor planning
22	mCingInsN	performance monitoring	response conflict
23	L-InsFPN	phonological working memory	working memory storage
24	BGN	reward anticipation	monetary reward prediction error
25	R-PcN	movement (left hand)	movement
26	ON-03	n.s.	-
27	FTPN-02	reading, mental arithmetic	word order
28	med-FN	theory of mind	inference
29	ON-02	visual form discrimination	task difficulty
30	D-FPN-02	motor imagery	movement
31	R-FInsN	interference resolution	cognitive control
32	OTN	object perception	visual object recognition
33	TN-02	speech perception	auditory sentence comprehension

The cognitive labels are based on the results of the meta-analytic cognitive decoding and were attributed by six independent authors ("Experts") or using a latent semantic analysis approach ("Latent semantic analysis") (see "Methods"). The anatomical nomenclature is described in the methods section. Abbreviations: *BG* basal ganglia, *a/m/pCing* anterior/middle/posterior cingulate, *D* dorsal, *F* frontal, *Ins* insular, *L* left, *med* median, *N* network, *n.s.* non-significant, *O* occipital, *P* parietal, *Pc* pericentral, *R* right, *T* temporal.

selective spatial attention corresponds to the dorsal frontoparietal network linked to attention. mCingInsN—RSN22, which is associated with performance monitoring, resembles the MidCingulo-Insular network[11], commonly referred to as the salience network. Performance monitoring implies detecting errors and conflicts during tasks and signaling the need for cognitive control adjustments, a role that seems in accordance with the functional definition of the salience network[40,41].

For a set of regions to be significantly associated with a given cognitive process, it is important that this association exhibits some specificity for this process: any set of regions that would systematically engage in many other tasks could lose its specificity and fail to be significantly more associated to a term than the others. Interestingly, this was the case for three networks (pCing-medPN—RSN01, R-FTPN-03—RSN02, and ON-3—RSN26). The fact that two of these networks were the most consistently detected RSNs across all individuals may indicate their prime importance in diverse cognitive activities, although their exact contribution remains to be determined. pCingmedPN is a dorsal module of the classically defined default-mode network[42], consistent with the reported role of the posterior cingulate cortex as a critical hub for the integration between multiple functional systems[43], and R-FTPN-03 shows substantial overlap with the 'Multiple Demand (MD) system'[44], although the latter is usually reported as bilateral rather than right-lateralized as in our case.

A detailed investigation of the terms decoded for well-studied networks, namely, default mode and language networks, highlights the precision of the method and its accordance with the literature. The cognitive labels that we associated with the default mode network (DMN) in its canonical definition (here, med-FPN—RSN07), almost exactly match the cognitive functions reported to be associated with increased activity within its nodes, namely autobiographical memory, self-referential cognition, and theory of mind, as recently reviewed[42].

The three networks that we uncover as related to language processes (L-FTN—RSN15, L-FTPN-01—RSN19, TN-02—RSN33) summarize well the current state of knowledge of the brain supports of language processes and reveal the superiority of the meta-analytic decoding over visual attribution of function. Indeed, though they share a consequent amount of overlap, each RSN's unique topographical pattern allows the segregation of their associated processes. Despite the overlap in the left superior temporal gyrus (STG), only TN-02—RSN33 is bilateral and, therefore, is associated with more perceptual aspects of speech, in line with the highest phonological specificity for the bilateral STG[45]. L-FTPN-01—RSN19, which we associate with sentence comprehension, encompasses regions situated along the inferior bank of the superior temporal sulcus, the temporal pole, the angular gyrus, the left frontal pole, and the left superior frontal gyrus, all reported to be associated with semantic processing[45]. This network is very similar to the core network of the SENtence Supramodal Areas AtlaS (SENSAAS), describing the essential areas for sentence reading, listening, and production[46].

The present work is not without limitations. Our approach inherits all shortcomings from performing decoding from a meta-analytic database of task studies. Namely, our study is anchored in the risks associated with reverse inference: it cannot be concluded that because a cognitive process P engages a given brain region R, the activity in R implies the presence of the cognitive process P[47]. In other terms, inferring cognitive processes to RSNs by analyzing their spatial similarity with task activations does not provide evidence of an explanatory relationship but rather, of a coarse associative one[48]. Relatedly, the distribution of cognitive terms inherently reflects how different cognitive domains are studied and reported by investigators, making them prone to an imbalance in how these domains are represented in the meta-analytic database (i.e., epistemological bias)[31].

Other limitations relate to the nature of the maps in the Neurosynth database. First, all task-fMRI studies proceed by contrasting some condition of interest to a control condition. By relying on this assumption of pure insertion[49,50], any process that would be shared by the task of interest and the control condition would be masked out. Second, even if we assumed that the terms extracted by Neurosynth purely reflect the cognitive concept of interest, the coordinates extraction is not selective. It means that all coordinates reported in the article will be extracted, irrespective of whether the different tables refer to results for different concepts. Although the statistic of Neurosynth association test maps assesses whether a given voxel is consistently reported active in studies that report the term of interest as compared to studies that do not, cognitive terms/concepts that systematically co-occur with the term of interest could muddy its obtained brain substrate.

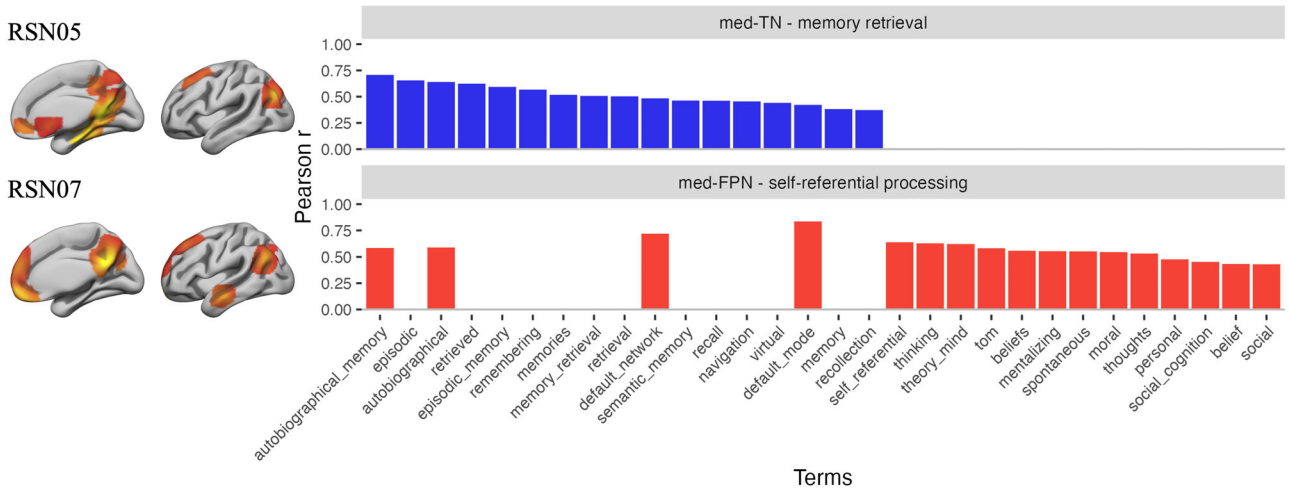

Fig. 4 | Decoding for default mode-related networks. The bar plots represent the Pearson correlations between each network related to the terms "default mode" /"default network" and the meta-analytic maps that show significance after correction for multiple comparisons ($p_{fwer} < 0.05$). Abbreviations: F frontal, med medial, N network, P parietal, T temporal.

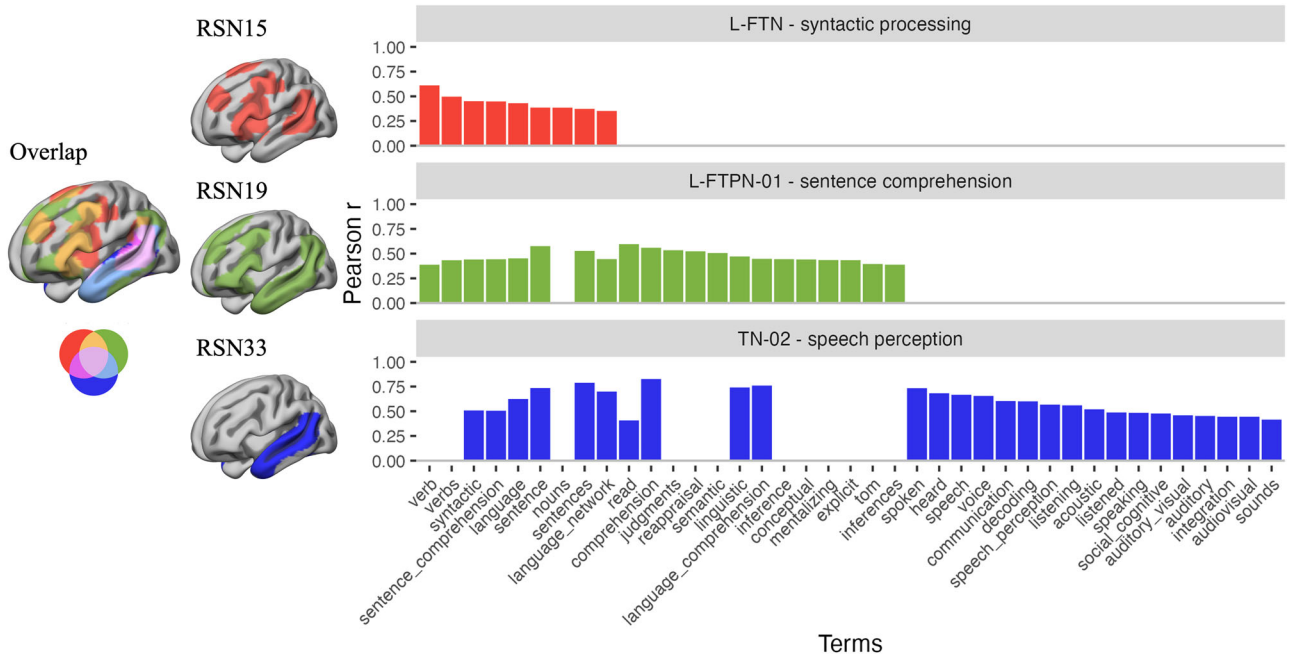

Fig. 5 | Decoding for language-related networks. The bar plots represent the Pearson correlations between each network related to the term "language" and the meta-analytic maps that show significance after correction for multiple comparisons ($p_{fwer} < 0.05$). The overlap between RSNs is illustrated (left brain image): all three RSNs overlap in the dorsal part of the left superior temporal gyrus and the posterior part of the superior temporal sulcus; L-FTN (top) and L-FTPN-01 (middle) partially overlap in the inferior frontal gyrus, precentral sulcus, and superior frontal gyrus. Abbreviations: F frontal, L left, N network, P parietal, T temporal.

Last, whether Neurosynth terms lie at the same level of description is not controlled and, due to the lack of specification of the ontological relationship between terms, cannot be determined. This complicates the choice of the appropriate level at which to assign a cognitive process to a network (e.g., visual perception vs. visual form discrimination).

Moreover, most task-based studies report results at the level of a restricted set of active brain regions or regions of interest. As our observed correlations rarely indicate a near-perfect match between RSNs and meta-analytic maps, our analysis does not allow us to firmly determine that the decoded processes are supported at the whole-network level, as opposed to a (subset of) region-level. The neural context hypothesis proposed that the functional relevance of a brain region relies on its co-activation with other brain regions[3]. This means that a given region, reported to be implicated in, e.g., working memory, may perform markedly different computations when inscribed in a larger network comprising regions related to, e.g., language. Similarly, there is no guarantee that discrete cognitive processes map onto discrete brain representations. Therefore, it remains to be determined whether RSNs correspond to the prospective exploration of specific cognitive functions or, alternatively, to lower-level "cognitive building blocks" that cannot be isolated from the contrast logic.

As establishing the relationship between the terms would necessitate a cognitive ontology[49,51] that has yet to emerge despite significant efforts pushed in that direction (the most developed one being the Cognitive Atlas[37]), we decided to rely on the qualitative attribution of networks' cognitive labels based on an expert consensus procedure. As a consequence, and because there is to date no clear understanding of how distinct cognitive

processes relate to one another[49], there is no guarantee that a fully data-driven specification of a cognitive process from a set of cognitive terms, such as the latent semantic analysis-based labeling that we here contrast with our consensus-driven labeling, results in the adequate level of specification. Indeed, though both methods generally agree, it is not clear that the latent semantic analysis provides solutions at the correct hierarchical level of cognitive processes. For instance, for RSN28, the automatic label "inference" may appear satisfactory, but such a level of specificity fails to capture the fact that these inferences are anchored in social cognition and concern the beliefs and intentions of others as indicated by the correlating terms. Similarly, for RSN33, the latent semantic analysis-driven label (auditory sentence perception) presents a good correspondence with the cognitive atlas definition (ability to combine auditory words into a meaningful sentence unit), but such a level of specificity fails to capture explicitly the more perceptive aspects that led to a good correlation with terms such as "acoustic", "voice", "auditory" or "sounds". Inversely, for RSN31, "cognitive control" could be considered a higher-order domain encompassing the "interference resolution" process chosen by the experts. This, again, relates to the lack of specification regarding the relationships between cognitive processes. Conversely, it is equally important to recognize that judgments made by human experts regarding the underlying cognitive processes are not immune to error. While we have focused our efforts on summarizing the decoded terms to reduce subjective biases, this approach only partially mitigates these limitations. We, therefore, encourage readers to critically evaluate and compare their own interpretations of the inferred processes with those proposed here (see the GitHub repository[32]). To further support transparency and community involvement, we have aligned RSN labels with processes defined in the Cognitive Atlas[37]. This alignment not only provides a systematic framework but also ensures that our propositions are amenable to further validation through empirical testing. By fostering open dialog and collaboration, we hope to refine and improve the labeling of RSNs, making this atlas a more robust and dynamic resource for the research community.

At the methodological level, while choosing anterior-posterior encoding over left-right/right-left encoding has the advantage of reducing hemispheric distortions[35], therefore enhancing the study of lateralization, its downside is to cause signal loss in anterior regions, particularly the orbitofrontal cortex (OFC). The known implication of OFC in emotion-related processes[52] may explain why none were associated with GINNA RSNs and leaves further room for the identification of RSNs relevant to their brain support.

From the statistical standpoint, although we employed a method of spatial autocorrelation-preserving null hypothesis modeling that effectively reduces false positive rates as compared with spatial naive models (e.g., random shuffling of voxels), slightly inflated false positive rates may remain[53], leaving room for further methodological developments.

Finally, it is worth noting that the employed methodology does not account for the relevance of the dynamics in the expression of resting-state networks. Several studies have demonstrated that RSNs that appear over the course of relatively long resting-state acquisitions are, in fact, superordinate approximations of underlying dynamic states[54–56]. Therefore, the exact cognitive relevance of RSNs, seen as a prospective exploration of cognitive states[38], might be better understood in light of their instantaneous interactions with the rest of the brain, as observed at any given time.

Overall, we provide the Groupe d'Imagerie Fonctionnelle Network Atlas (GINNA), a 33 resting-state networks atlas of the human brain grounded in a meta-analytic decoding-based characterization of its cognitive relevance. Each resting-state network's cognitive relevance is provided in terms of well-defined cognitive processes taken from the Cognitive Atlas ontology, and, as such, should represent better guides for future investigations. The atlas covers a broad spectrum of the human cognitive repertoire, with processes that align with brain laterality and display high associative precision. Potential use cases for GINNA include the selection of a priori regions of interest belonging to a specific network for neuroimaging analyses in the absence of task-derived functional data acquisition, as well as using the maps to analyze a posteriori whether significant regions/edges are distributed within specific cognitive systems.

Methods

MRi-Share study protocol

All participants ($n = 1812$; 1304 females (71.96%), 508 males (28.04%); mean age ± s.d.: 22.10 ± 2.29) were part of MRi-Share[35,57], the Magnetic Resonance Imaging (MRI)-based substudy of the larger internet-based Students Health Research Enterprise (i-Share) cohort, launched in 2013. Detailed study protocol, demographic information and methodological description are available in Tsuchida et al. (2021)[35].

Ethics approval

All procedures were performed in compliance with the declaration of Helsinki, and were approved by the Comité de Protection des Personnes Sud-Ouest et Outre-Mer (local ethics committee CPP SOOMIII) with agreement nr 2015-A00850-49. All ethical regulations relevant to human research participants were followed.

Consent to participate

All participants signed an informed written consent form.

Resting-state fMRI acquisition

All neuroimaging data were acquired between November 2015 and November 2017. Participants underwent a single run of resting-state echo-planar imaging (EPI) functional MRI (fMRI) acquisition (Siemens 3 T Prisma, 64-channels head coil; voxel size: $2.4 \times 2.4 \times 2.4$ mm^3; Time of Repetition (TR) = 850 ms; Time of Echo (TE) = 35.0 ms; flip angle = 56°, multi-band factor = 6), for a duration of approximately 15 min. This resulted in 1054 brain volumes acquired for each participant. Prior to the resting-state fMRI (rs-fMRI) acquisition, participants were instructed to "keep their eyes closed, to relax, to refrain from moving, to stay awake, and to let their thoughts come and go". Additionally, left-right and right-left phase encoding, as used in some studies, has been shown to cause voxel displacement between runs, even after phase correction, leading to hemispheric distortions[35]. Since hemispheric lateralization is critical for studying human cognition, we avoided such distortions by acquiring whole-brain images in the axial direction with an antero-posterior phase encoding, a design choice also adopted by the UK Biobank cohort[58]. In addition to the resting-state acquisition, other imaging modalities were acquired, including T1-weighted (T1w) structural images (one volume; three-dimensional Magnetization Prepared Rapid Gradient Echo (3D MPRAGE) sequence; Siemens 3 T Prisma, 64-channels head coil; voxel size: $1.0 \times 1.0 \times 1.0$ mm^3; Time of Repetition (TR) = 2000 ms; Time of Echo (TE) = 2.0 ms; Time of Inversion = 880 ms). In total, a whole acquisition session lasted for approximately 45 min.

Resting-state fMRI preprocessing

The preprocessing pipeline is described in detail in the supplementary materials of Tsuchida et al.[35]. Briefly, the distortion-corrected rs-fMRI data were registered to anatomical space, spatially filtered with a Gaussian full width at half maximum of 5 mm in each orthogonal dimension, and time band-pass filtered to a frequency window of 0.01–0.1 Hz. Images were subsequently registered to the Montreal Neurological Institute (MNI) standard space (sampling of $2 \times 2 \times 2$ mm^3). The temporal signal was corrected from the movement parameters and their derivatives, as well as the average of the signal recorded in the white matter, cerebrospinal fluid, and gray matter (global signal regression). Preprocessing primarily involved tools from FSL v5.0.10[59] and AFNI v10.0.05[60] encapsulated into a singularity container.

GINNA resting state Atlas

Briefly, the three steps of the GINNA atlas creation are as follows: (1) Subject individual independent component (IC) analysis (ICA), (2) ICs classification into 41 classes, and (3) Atlas creation.

(1) *Subject-level independent component analysis*. Individual fMRI data were processed using the ICA program MELODIC (multivariate exploratory linear optimized decomposition into independent components, version

3.14) available in FSL[59]. For each subject, the number of ICs was estimated using the Laplace approximation[61].

(2) *ICs classification into 41 classes*. This was done using the MICCA clustering algorithm[62], Icasso[63], and supervised deep learning-based classification of ICs[64]. The MICCA algorithm (Multi-scale Individual Component Clustering) proceeds in three stages: (i) creation of a cluster of individual independent components (cIC) grouping all pairs of ICs having a similarity value higher than a threshold (sc), (ii) iterative merging of cICs, and (iii) iterative (re-) classification of misclassified ICs. The similarity between pairs of ICs was computed using the Pearson correlation coefficient (see Eq. 1 in Naveau et al. (2012)[62]). The sc threshold is defined on bi-modal Gaussian modeling of the distribution of the maximum absolute similarity value of each independent component. This threshold defines which components are either included in or excluded from the considered cIC based on a pairwise similarity criterion. The pairs to include are selected among the set of all pairs of ICs. The first step is an agglomerative clustering which self-determines the number of clusters, the second step agglomerates clusters that show high similarity (each cluster is characterized by the average t-map of the ICs belonging to the cluster) and were composed from different subjects. The variability is accounted for by repeatedly running the MICCA algorithm on 42 subsets of subjects. The whole set is divided randomly into 6 subsets (~302 different subjects per subset) and the procedure is repeated 7 times. Overall, each IC was included in 7 analyses. After removing clusters with less than 20% of the subjects, the resultant clusters (2154 on average 51 groups per repetition) are processed using the ICASSO method as implemented by Himberg et al. (2003)[63]. Classes of cluster corresponding to the same spatial signal sources are grouped on the basis of their t-map similarity indices, producing a tree-like hierarchy (dendrogram) of the clusters. Follows an iterative analysis of the dendrogram to extract groups of classes including at least 75% of the repetitions that led to a definition of 41 classes. Using a maximum voting scheme across the 7 iterations, each selected IC was affected by one of the 41 classes. The last step involved a deep-learning-based classification of ICs into the 41 classes defined following the ICASSO procedure. The goal of adding the deep learning-based classification was first to increase the robustness of the classification, as the classification was based on the IC voxel values and not only on the similarity between pairs of ICs. The second goal was to smooth the abrupt cut-off (the sc; see below) that determined which ICs were included in the MICCA classification. After training from the MICCA output, all the ICs were classified (ICs excluded from the first analysis) or re-classified. For each ICs and each class, a score representing the probability for the ICs to belong to the class was predicted. The ICs were affected to the maximum value class if its value was above 0.95 and to a "noise" class otherwise.

(3) *Atlas creation*. for each class, the individual ICs were averaged to obtain a group-level IC map. This class map was thresholded by selecting voxels that belong to at least 50% of the individual ICs (individual z-maps thresholded using a mixture model of a Gaussian plus two gamma distributions at $p = 0.5$).

Decoding the cognitive terms associated with resting-state networks

The meta-analytic decoding procedure[65,66] is illustrated in Fig. 6. In order to decode the cognitive terms associated with each GINNA resting-state network (RSN), the extracted group-level IC maps of RSNs were spatially compared with meta-analytic activation maps (MAMs) extracted from the Neurosynth database[25]. Each MAM corresponds to a term used in the fMRI literature (e.g., fear) and aggregates results based on the coordinates of activation reported in all studies using the term at a frequency of at least 1/1000 words. As Neurosynth proceeds by an automatic scraping of the literature, the database includes terms not limited to cognitive behavioral denomination, such as anatomical (e.g., accumbens) or vague/broad terms (e.g., accurately). Therefore, we employed a subset of the Neurosynth database manually curated to be specifically representative of cognition[31,67]. This subset comprises 506 MAMs (association test maps), encompassing 11406 studies of the fMRI literature, published between 1999 and 2017.

Both RSN and thresholded MAMs ($z = 3.4$) were first parcellated using a combination of a first atlas for cortical and subcortical volume that accounts for homotopy, a major aspect of the human brain organization (AICHA V2)[68], and AAL3[69] for cerebellum. The choice of the AICHA atlas was motivated by (i) its creation from resting-state data, ensuring proximity in the nature of the present work's data, (ii) the definition of parcels based on their functional homogeneity during rest; (iii) the observation that a number of GINNA RSNs displayed lateralization, justifying the use of a region-level

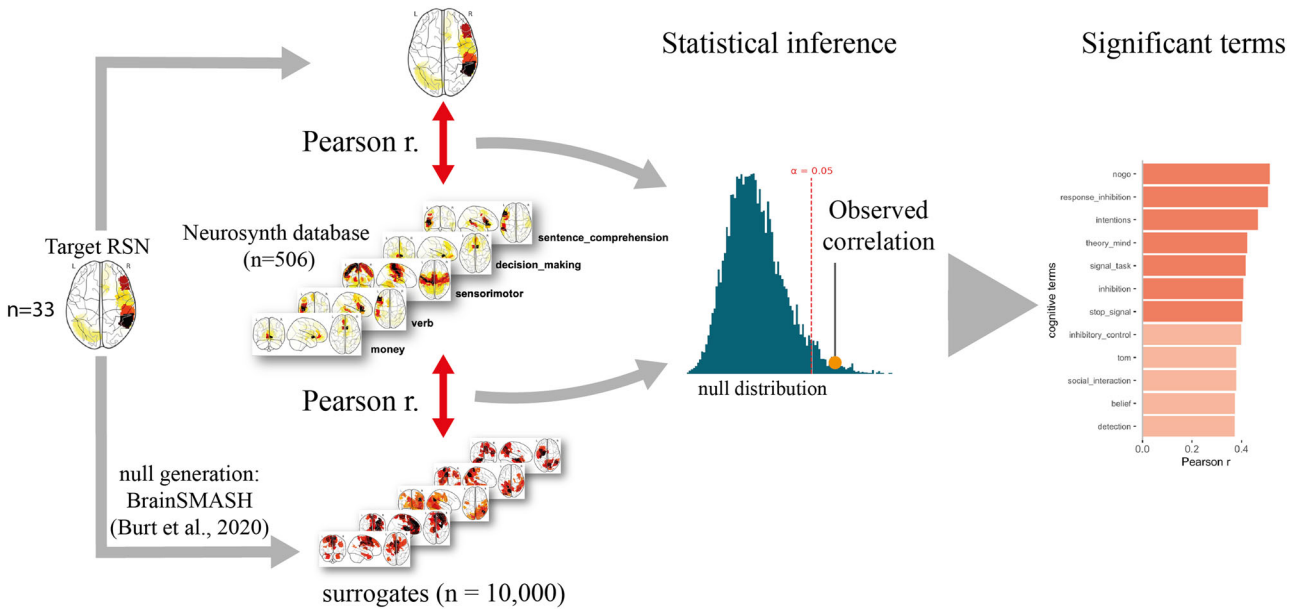

Fig. 6 | Meta-analytic decoding of cognitive terms. Each considered resting-state network was spatially compared to a manually curated subset of the Neurosynth database using Pearson correlation as a metric. The procedure was repeated for a population of 10,000 surrogate maps generated using the BrainSMASH package (see "Methods"), yielding a distribution of spatial similarity that would be observed by chance. Each network was associated with the terms whose corresponding maps were significantly correlated with the database ($p < 0.05$ after family-wise error rate correction for multiple comparisons).

parcellation well suited for the study of hemispheric specialization[68]. For each brain map, the average value of all voxels within each parcel was extracted using the Nilearn object NiftiLabelMasker, resulting in 410 values. A spatial comparison of each vectorized RSN map to the Neurosynth database was performed by computing Pearson product-moment correlations between each resting-state network/meta-analytic map pair, resulting in 506 correlations for each of the considered RSNs. The use of Pearson correlation, as opposed to similarity measures operating on binarized maps (e.g., Dice coefficient), aimed at considering both the topographical aspect of maps (which parcels do they cover) as well as the distribution of the *z*-scores values (how strongly are parcels associated with each map).

In order to determine the statistical significance of the correlation between an input RSN map and the meta-analytic maps of the database, we implemented a procedure of generative null hypothesis testing. Namely, for each RSN, we computed a null distribution of 10,000 autocorrelation-preserving surrogate maps using the BrainSmash package[70] as implemented in Python (https://brainsmash.readthedocs.io). Information about the distance between brain regions was calculated using the Euclidean distance[70] and provided to the software as a 410×410 distance matrix. Spatial autocorrelation has been identified as a key component of brain organization. Taking it into account in the null hypothesis modeling effectively leads to consequent false positive rate reduction as compared to spatially-unconstrained surrogates[71].

The Pearson product-moment correlations between each surrogate map and the database were computed, leading to a distribution of null correlations for each term, further allowing us to compare the observed correlation value for the considered term to those that would be observed by chance ($506 \times 10{,}000$). To account for multiple comparisons, the maximal correlation across all terms was retained for each exemplar of the null distribution, resulting in a null distribution ($n = 10{,}000$) accounting for family-wise error rate (fwer). This null distribution was used to determine the MAMs that were significantly correlated with the considered RSN ($p_{fwer} < 0.05$). The terms corresponding to the MAMs significantly correlated with the RSNs were further extracted, effectively resulting in the association of RSNs to one or several (if any) cognitive terms.

Identification of RSNs principal "cognitive" components

We performed a principal component analysis (PCA) at the single RSN level as a complementary analysis to better understand their cognitive fingerprint. The 506 terms extracted from Neurosynth and their associated Meta-Analytic Maps refer to concepts that are not independent of each other and are, in fact, sometimes extremely close. For example, terms such as 'comprehension', 'sentence', 'language comprehension', 'linguistic', 'speech', 'spoken', or 'voice' overlap at a conceptual or paradigmatic level. This proximity results in spatial proximity of the MAMs, where similar brain regions are engaged because the cognitive processes involved do overlap. We used PCA to capture these similarities and thus discover the latent features leading to a significant association between the terms and the RSNs. Knowing which terms load particularly high on a given dimension increases its interpretability and allows to generalize its contribution beyond the use of single isolated terms. Interestingly, a by-product of this analysis concerns the possibility of projecting each dimension loading back to the brain regions, as it indicates what regions of the networks present the highest loadings for a given dimension.

We first retrieved the parcellated MAMs that were significantly associated with the target RSN, and, for each of them, extracted z-score values of parcels associated with the RSN. In order to do so, we created a binary mask of the parcellated versions of the RSN by considering a parcel as belonging to an RSN if it exceeded a liberal *z*-score threshold of 1. To consider only RSN-relevant regions, parcellated MAMs were further masked with their respective vectorized RSN mask. PCA was computed using the R FactoMineR package[72], by treating individual brain regions composing the network as samples, parametrized by their activation values across the set of significantly associated term meta-analytic maps. From the PCA, we retrieved the percentage of explained variance of each component. To assess the contribution of both cognitive terms and brain regions to each component, their coordinates were extracted. Coordinates for cognitive terms were ordered to reveal the terms that were the most representative of the component. PCA was not computed for RSNs with less than three significantly associated MAMs.

Anatomical nomenclature

Following guidelines of the Organization for Human Brain Mapping (OHBM) Workgroup for HArmonized Taxonomy of NETworks (WHATNET) consortium[12], we did not restrict the labeling of GINNA RSNs to cognitive terminology but grounded it into an anatomical taxonomy. This is to prevent any confusion regarding the identification of GINNA RSNs, which are mainly referred to by their anatomical description and then supplemented with their suggested cognitive relevance. RSNs anatomical nomenclature comprised the cerebral lobes (Frontal (F), Temporal (T), Parietal (P), Occipital (O), Cingular (Cing), Insular (Ins)), as well as the pericentral sulcus (Pericentral (Pc)) and subcortical nuclei (basal ganglia, BG). The cingulum was specified with a, m, and *p* (for anterior, mid, and posterior). A lobe was included in the nomenclature of a given RSN if it contained voxels among the 50% highest *z*-values of the RSN maps. In addition, a left or right lateralization (L/R, respectively), Dorsal (D), and medial (med) indicator was added as a prefix to the anatomical nomenclature when relevant. In cases where multiple RSNs were attributed the same anatomical nomenclature, a numbering following the principal gradient of cortical connectivity extending from low-level, unimodal sensory cortices up to higher-level, heteromodal association cortices[65] was added as a suffix.

Consensus cognitive labeling

Because the terms present in the Neurosynth database are uncontextualized, having meta-analytic terms significantly associated with resting-state networks is not sufficient to assign to them one or multiple cognitive processes. A term such as 'face', for instance, could indeed be reliably reported in studies about the somatomotor homonculus of the face, their visual perception, or because they are the support of an emotion recognition task. For this reason, we decided to resort to a qualitative attribution of cognitive processes to RSNs by neuroimaging experts. Six authors were asked to independently attribute one or several cognitive processes to the networks. All answers were collected via an online questionnaire. The experts were trained in cognitive psychology ($N = 2$), psychiatry ($N = 1$), cognitive neuroscience ($N = 2$) and signal processing ($N = 1$). All have at least 25 years of professional experience (except for the first author, who is a PhD student) and have an established track record of publications in the field of cognitive neuroimaging. Each expert's labeling of RSNs was based on the set of significantly associated terms, their strength of correlation, and the results of PCA, and they were asked to rely as little as possible on the spatial distribution of the parcels. Each expert sought individually to identify a cognitive process/function based on the above-mentioned information. To do so, they relied on their knowledge of the typical experimental tasks or stimuli used in relation to a given process, on their interpretation of principal components revealed by the PCA, and on the contextualization of the terms by the location of the associated parcels (e.g., "movement" associated tothe right or left hand, or "matching" associated with visual cortex). In each case, the experts discussed the data and reached a consensus on the cognitive function(s) represented. The most representative term was then selected from the Cognitive Atlas (https://cognitiveatlas.org/), and its definition was verified to align with the consensus.

Latent semantic cognitive labeling

We performed a latent semantic analysis to identify the cognitive processes with the highest conceptual similarity with terms decoded for each RSN, as reflected in how they are used in the fMRI literature. Previous approaches addressing the data-driven identification of cognitive domains have proposed to name domains according to their most representative Neurosynth terms[73]. However, in contrast to this approach, and in line with our goal of

preserving the complexity of Resting State Network (RSN) functions, we adopted a different strategy. Specifically, we sought to identify the Cognitive Atlas process that exhibited the highest conceptual similarity to the RSN, as determined through latent semantic analysis of the decoded Neurosynth terms associated with it.

We thus created a corpus of documents from the fMRI literature by extracting titles and abstracts of articles included in the Neurosynth database, using the NiMARE v 0.1.1 package implemented in Python 3.11.5. This resulted in the extraction of 14371 documents. From this corpus, we created a term frequency-inverse document frequency (tf-idf) matrix of dimensions (n_words, n_documents) using the class TfidfTransformer applied to the output of CountVectorizer with a word frequency cutoff of 0.001 (similar to Neurosynth), implemented in scikit-learn v 1.3.1.

We preprocessed the set of Neurosynth terms corresponding to the MAMs used in this study ($n = 506$), and the cognitive processes available in the Cognitive Atlas (obtained from web scraping ($n = 521$)), using tokenization and stemming. (e.g., "speech perception" was decomposed into two tokens ["speech", "percept"]). As we set a frequency threshold of 0.001, it was not guaranteed that all relevant terms would be included in the count matrix. We, therefore, checked that all tokens ($n = 568$) were included in the CountVectorizer vocabulary. 20 tokens were missing and, as a consequence, were manually appended to the existing vocabulary. The CountVectorizer and TfidfTransformer were subsequently refit.

These steps resulted, for each selected term, in an abstract vector representation based on how they are used in the literature. Therefore, vectors that are highly similar are used in similar articles, reflecting a conceptual similarity. These vectors were embedded into a lower-dimensional representation using singular value decomposition implemented as TruncatedSVD in scikit-learn. This resulted in embeddings for cognitive terms/processes of dimension 500.

To associate a given RSN to a Cognitive Atlas process, we first calculated the RSN "conceptual" representation by extracting all its significantly associated terms, and by computing the average of their embedding vectors weighted by their corresponding similarity with the RSN (Pearson r). This is to ensure that the more strongly associated terms with an RSN (as assessed by the Pearson correlation coefficient) contribute proportionally more to the RSN vector representation. Finally, the cognitive atlas process with the highest cosine similarity in the embedding space was extracted and associated with the RSN.

Statistics and reproducibility

Statistical assessments conducted for each step of the RSNs creation and cognitive labeling are detailed in their relevant subsections in the Methods. All information regarding participants' demographics, study design, and data analyses that allow full reproducibility are provided in the Methods and Code availability sections.

Reporting summary

Further information on research design is available in the Nature Portfolio Reporting Summary linked to this article.

Data availability

The GINNA atlas is available at https://github.com/Achillegillig/ginna[32]. Due to French regulations regarding sharing of the medical imaging data, individual raw data used for this study cannot be shared through a public repository. Rather, for MRi-Share de-identified data[35,57], a request can be submitted to the i-Share Scientific Collaborations Coordinator (ilaria.montagni@ubordeaux.fr), the procedure is described on the i-Share web site (https://research.i-share.fr/).

Code availability

The code is made available in the GINNA github repository (https://github.com/Achillegillig/ginna[32]). Analyses are provided as Jupyter notebooks and allow for full reproducibility of the present results.

Received: 25 July 2024; Accepted: 4 February 2025;
Published online: 18 February 2025

References

1. Biswal, B., Zerrin Yetkin, F., Haughton, V. M. & Hyde, J. S. Functional connectivity in the motor cortex of resting human brain using echo-planar MRI. *Magn. Reson. Med.* **34**, 537–541 (1995).
2. Goldman-Rakic, P. S. Topography of cognition: parallel distributed networks in primate association cortex. *Annu. Rev. Neurosci.* **11**, 137–156 (1988).
3. McIntosh, A. R. Towards a network theory of cognition. *Neural Netw.* **13**, 861–870 (2000).
4. Mesulam, M.-M. Large-scale neurocognitive networks and distributed processing for attention, language, and memory. *Ann. Neurol.* **28**, 597–613 (1990).
5. Hampson, M., Olson, I. R., Leung, H.-C., Skudlarski, P. & Gore, J. C. Changes in functional connectivity of human MT/V5 with visual motion input. *NeuroReport* **15**, 1315 (2004).
6. Vincent, J. L. et al. Coherent spontaneous activity identifies a hippocampal-parietal memory network. *J. Neurophysiol.* **96**, 3517–3531 (2006).
7. Cordes, D. et al. Mapping functionally related regions of brain with functional connectivity MR imaging. *Am. J. Neuroradiol.* **21**, 1636–1644 (2000).
8. Damoiseaux, J. S. et al. Consistent resting-state networks across healthy subjects. *Proc. Natl Acad. Sci. USA* **103**, 13848–13853 (2006).
9. De Luca, M., Beckmann, C. F., De Stefano, N., Matthews, P. M. & Smith, S. M. fMRI resting state networks define distinct modes of long-distance interactions in the human brain. *NeuroImage* **29**, 1359–1367 (2006).
10. Fox, M. D. & Raichle, M. E. Spontaneous fluctuations in brain activity observed with functional magnetic resonance imaging. *Nat. Rev. Neurosci.* **8**, 700–711 (2007).
11. Uddin, L. Q., Yeo, B. T. T. & Spreng, R. N. Towards a Universal Taxonomy of Macro-scale Functional Human Brain Networks. *Brain Topogr.* **32**, 926–942 (2019).
12. Uddin, L. Q. et al. Controversies and progress on standardization of large-scale brain network nomenclature. *Netw. Neurosci.* **7**, 864–905 (2023).
13. Fox, M. D. et al. The human brain is intrinsically organized into dynamic, anticorrelated functional networks. *Proc. Natl Acad. Sci. USA* **102**, 9673–9678 (2005).
14. Doucet, G. et al. Brain activity at rest: a multiscale hierarchical functional organization. *J. Neurophysiol.* **105**, 2753–2763 (2011).
15. Yeo, B. T. T. et al. The organization of the human cerebral cortex estimated by intrinsic functional connectivity. *J. Neurophysiol.* **106**, 1125–1165 (2011).
16. Thompson, W. H. & Fransson, P. Spatial confluence of psychological and anatomical network constructs in the human brain revealed by a mass meta-analysis of fMRI activation. *Sci. Rep.* **7**, 44259 (2017).
17. Smith, S. M. et al. Correspondence of the brain's functional architecture during activation and rest. *Proc. Natl Acad. Sci. USA* **106**, 13040–13045 (2009).
18. Fox, P. T. et al. Brainmap taxonomy of experimental design: Description and evaluation. *Hum. Brain Mapp.* **25**, 185–198 (2005).
19. Cole, M. W., Ito, T., Bassett, D. S. & Schultz, D. H. Activity flow over resting-state networks shapes cognitive task activations. *Nat. Neurosci.* **19**, 1718–1726 (2016).
20. Cole, M. W., Bassett, D. S., Power, J. D., Braver, T. S. & Petersen, S. E. Intrinsic and task-evoked network architectures of the human brain. *Neuron* **83**, 238–251 (2014).
21. Bertolero, M. A., Yeo, B. T. T. & D'Esposito, M. The modular and integrative functional architecture of the human brain. *Proc. Natl Acad. Sci. USA* **112**, E6798–E6807 (2015).
22. Yeo, B. T. T. et al. Functional specialization and flexibility in human association cortex. *Cereb. Cortex* **25**, 3654–3672 (2015).

23. Laird, A. R. et al. Behavioral interpretations of intrinsic connectivity networks. *J. Cogn. Neurosci.* **23**, 4022–4037 (2011).
24. Anderson, M. L., Kinnison, J. & Pessoa, L. Describing functional diversity of brain regions and brain networks. *NeuroImage* **73**, 50–58 (2013).
25. Yarkoni, T., Poldrack, R. A., Nichols, T. E., Van Essen, D. C. & Wager, T. D. Large-scale automated synthesis of human functional neuroimaging data. *Nat. Methods* **8**, 665–670 (2011).
26. Poldrack, R. A. Inferring mental states from neuroimaging data: from reverse inference to large-scale decoding. *Neuron* **72**, 692–697 (2011).
27. Poldrack, R. A., Halchenko, Y. O. & Hanson, S. J. Decoding the large-scale structure of brain function by classifying mental states across individuals. *Psychol. Sci.* **20**, 1364–1372 (2009).
28. Rubin, T. N. et al. Decoding brain activity using a large-scale probabilistic functional-anatomical atlas of human cognition. *PLOS Comput. Biol.* **13**, e1005649 (2017).
29. Wegrzyn, M. et al. Thought experiment: Decoding cognitive processes from the fMRI data of one individual. PLOS ONE **13**, e0204338 (2018).
30. Boeken, O. J. & Markett, S. Systems-level decoding reveals the cognitive and behavioral profile of the human intraparietal sulcus. *Front. Neuroimaging* **1**, 1074674 (2023).
31. Pacella, V. et al. The morphospace of the brain-cognition organisation. Nat Commun **15**, 8452 (2024).
32. Gillig, A. Code for: GINNA, a 33 resting-state networks atlas with meta-analytic decoding-based cognitive characterization. *Zenodo* https://doi.org/10.5281/zenodo.14732372 (2025).
33. Du, Y. P., Dalwani, M., Wylie, K., Claus, E. & Tregellas J. R. Reducing susceptibility artifacts in fMRI using volume-selective z-shim compensation. *Magn. Reson. Med.* **57**, 396–404 (2007).
34. Lamberton, F., Delcroix, N., Grenier, D., Mazoyer, B. & Joliot, M. A new EPI-based dynamic field mapping method: Application to retrospective geometrical distortion corrections. *J. Magn. Reson. Imaging* **26**, 747–755 (2007).
35. Tsuchida, A. et al. The MRi-Share database: brain imaging in a cross-sectional cohort of 1870 university students. *Brain Struct. Funct.* **226**, 2057–2085 (2021).
36. Smith, S. M. et al. Resting-state fMRI in the Human Connectome Project. *NeuroImage* **80**, 144–168 (2013).
37. Poldrack, R. et al. The Cognitive Atlas: toward a knowledge foundation for cognitive neuroscience. *Front. Neuroinform.* **5**, (2011).
38. Deco, G., Jirsa, V. K. & McIntosh, A. R. Resting brains never rest: computational insights into potential cognitive architectures. *Trends Neurosci.* **36**, 268–274 (2013).
39. Jabakhanji, R. et al. Limits of decoding mental states with fMRI. *Cortex* **149**, 101–122 (2022).
40. Seeley, W. W. The salience network: a neural system for perceiving and responding to homeostatic demands. *J. Neurosci.* **39**, 9878–9882 (2019).
41. Seeley, W. W. et al. Dissociable intrinsic connectivity networks for salience processing and executive control. *J. Neurosci.* **27**, 2349–2356 (2007).
42. Menon, V. 20 years of the default mode network: a review and synthesis. *Neuron* **111**, 2469–2487 (2023).
43. Leech, R., Braga, R. & Sharp, D. J. Echoes of the brain within the posterior cingulate cortex. *J. Neurosci.* **32**, 215–222 (2012).
44. Duncan, J. The structure of cognition: attentional episodes in mind and brain. *Neuron* **80**, 35–50 (2013).
45. Turker, S., Kuhnke, P., Eickhoff, S. B., Caspers, S. & Hartwigsen, G. Cortical, subcortical, and cerebellar contributions to language processing: a meta-analytic review of 403 neuroimaging experiments. *Psychol. Bull.* **149**, 699–723 (2023).
46. Labache, L. et al. A SENtence Supramodal Areas AtlaS (SENSAAS) based on multiple task-induced activation mapping and graph analysis of intrinsic connectivity in 144 healthy right-handers. *Brain Struct. Funct.* **224**, 859–882 (2019).
47. Poldrack, R. Can cognitive processes be inferred from neuroimaging data? *Trends Cogn. Sci.* **10**, 59–63 (2006).
48. Mill, R. D., Ito, T. & Cole, M. W. From connectome to cognition: the search for mechanism in human functional brain networks. *NeuroImage* **160**, 124–139 (2017).
49. Poldrack, R. A. & Yarkoni, T. From brain maps to cognitive ontologies: informatics and the search for mental structure. *Annu. Rev. Psychol.* **67**, 587–612 (2016).
50. Sternberg, S. Memory-scanning: mental processes revealed by reaction-time experiments. *Am. Sci.* **57**, 421–457 (1969).
51. Francken, J. C., Slors, M. & Craver, C. F. Cognitive ontology and the search for neural mechanisms: three foundational problems. *Synthese* **200**, 378 (2022).
52. Rolls, E. T. Emotion, motivation, decision-making, the orbitofrontal cortex, anterior cingulate cortex, and the amygdala. *Brain Struct. Funct*. https://doi.org/10.1007/s00429-023-02644-9 (2023).
53. Markello, R. D. & Misic, B. Comparing spatial null models for brain maps. *NeuroImage* **236**, 118052 (2021).
54. Ciric, R., Nomi, J. S., Uddin, L. Q. & Satpute, A. B. Contextual connectivity: a framework for understanding the intrinsic dynamic architecture of large-scale functional brain networks. *Sci. Rep.* **7**, 6537 (2017).
55. Sporns, O., Faskowitz, J., Teixeira, A. S., Cutts, S. A. & Betzel, R. F. Dynamic expression of brain functional systems disclosed by fine-scale analysis of edge time series. *Netw. Neurosci.* **5**, 405–433 (2021).
56. Tagliazucchi, E., Balenzuela, P., Fraiman, D. & Chialvo, D. R. Criticality in large-scale brain fMRI dynamics unveiled by a novel point process analysis. *Front. Physiol*. **3**, 15 (2012).
57. Crivello, F., Tsuchida, A., Mazoyer, B. & Tzourio, C. Data from: The MRi-Share database: Brain imaging in a cross-sectional cohort of 1,870 university students. *Dryad* https://doi.org/10.5061/DRYAD.Q573N5TJ2 (2022).
58. Alfaro-Almagro, F. et al. Image processing and Quality Control for the first 10,000 brain imaging datasets from UK Biobank. *NeuroImage* **166**, 400–424 (2018).
59. Smith, S. M. et al. Advances in functional and structural MR image analysis and implementation as FSL. *NeuroImage* **23**, S208–S219 (2004).
60. Cox, R. W. AFNI: software for analysis and visualization of functional magnetic resonance neuroimages. *Comput. Biomed. Res. Int. J.* **29**, 162–173 (1996).
61. Minka, T. Automatic choice of dimensionality for PCA. in *Advances in Neural Information Processing Systems* (eds Leen, T., Dietterich, T. & Tresp, V.) vol. 13 (MIT Press, 2000).
62. Naveau, M. et al. A Novel Group ICA approach based on multi-scale individual component clustering. Application to a large sample of fMRI data. *Neuroinformatics* **10**, 269–285 (2012).
63. Himberg, J. & Hyvarinen, A. Icasso: software for investigating the reliability of ICA estimates by clustering and visualization. in *2003 IEEE XIII Workshop on Neural Networks for Signal Processing (IEEE Cat. No.03TH8718)* 259–268 (2003). https://doi.org/10.1109/NNSP.2003.1318025.
64. Nozais, V. et al. Deep Learning-based classification of resting-state fMRI independent-component analysis. *Neuroinformatics* **19**, 619–637 (2021).
65. Margulies, D. S. et al. Situating the default-mode network along a principal gradient of macroscale cortical organization. *Proc. Natl. Acad. Sci. USA* **113**, 12574–12579 (2016).
66. Peraza, J. A. et al. Methods for decoding cortical gradients of functional connectivity. *Imaging Neurosci.* **2**, 1–32 (2024).
67. Karolis, V. R., Corbetta, M. & Thiebaut De Schotten, M. The architecture of functional lateralisation and its relationship to

callosal connectivity in the human brain. *Nat. Commun.* **10**, 1417 (2019).
68. Joliot, M. et al. AICHA: An atlas of intrinsic connectivity of homotopic areas. *J. Neurosci. Methods* **254**, 46–59 (2015).
69. Rolls, E. T., Huang, C.-C., Lin, C.-P., Feng, J. & Joliot, M. Automated anatomical labelling atlas 3. *NeuroImage* **206**, 116189 (2020).
70. Burt, J. B., Helmer, M., Shinn, M., Anticevic, A. & Murray, J. D. Generative modeling of brain maps with spatial autocorrelation. *NeuroImage* **220**, 117038 (2020).
71. Markello, R. D. et al. neuromaps: Structural and functional interpretation of brain maps. *Nat. Methods* **19**, 1472–1479 (2022).
72. Lê, S., Josse, J. & Husson, F. FactoMineR: An *R* Package for Multivariate Analysis. *J. Stat. Softw*. **25**, (2008).
73. Beam, E., Potts, C., Poldrack, R. A. & Etkin, A. A data-driven framework for mapping domains of human neurobiology. *Nat. Neurosci.* **24**, 1733–1744 (2021).

Acknowledgements

Computer time for this study was provided by the computing facilities of the MCIA (Mésocentre de Calcul Intensif Aquitaine, Bordeaux, France). The i-Share cohort has been funded by a grant ANR-10COHO-05-01 (P.I. C Tzourio) as part of the Program pour les Investissements d'Avenir. Supplementary funding was received from the Conseil Régional of Nouvelle-Aquitaine, Reference 4370420 (P.I. C Tzourio). The MRi-Share cohort has been supported by grants ANR-10-LABX-57 (P.I. B Mazoyer) and ANR-16-LCV2-0006 (GINESISLAB for the software, P.I. M Joliot). The bio-Share cohort and some regulatory and ethical aspects of MRiShare have been supported by the European Research Council (ERC) under the European Union's Horizon 2020 research and innovation program under Grant Agreement No. 640643 (P.I.S. Debette) and the FHU SMART. Achille Gillig has benefited from state support managed by the Agence Nationale de la Recherche (French National Research Agency) under reference [17]-EURE-0028.

Author contributions

Conceptualization: M.J. and G.J.; Methodology: A.G., G.J., M.J., and S.C.; Formal analysis and investigation: A.G., G.J., M.J., S.C., E.M., and L.Z.; Writing—review and editing: A.G., G.J., M.J., S.C., L.Z., E.M., and M.T.; Supervision: M.J. and G.J.

Competing interests

Michel Thiebaut de Schotten is an Editorial Board Member for Communications Biology, but was not involved in the editorial review of, nor the decision to publish this article. The remaining authors declare no competing interests.

Additional information

Supplementary information The online version contains supplementary material available at https://doi.org/10.1038/s42003-025-07671-2.

Correspondence and requests for materials should be addressed to Marc Joliot.

Peer review information *Communications Biology* thanks Rebecca Jackson, Jianxiao Wu and the other, anonymous, reviewer(s) for their contribution to the peer review of this work. Primary Handling Editor: Jasmine Pan. A peer review file is available.